

# AEROPROPULSIVE CHARACTERIZATION OF THE HYPERSONIC CRUISER VEHICLE IN STRATOFLY PROJECT

P. Roncioni<sup>1</sup>, L. Cutrone<sup>1</sup>, M. Marini<sup>1</sup>

<sup>1</sup>CIRA - Centro Italiano di Ricerche Aerospaziali

## Abstract

The H2020 STRATOFLY Project is a highly-multidisciplinary project co-funded by the European Commission that combines technological and operative issues for hypersonic civil aircrafts and aims to study the feasibility of high-speed passenger stratospheric flight. The main objectives were to refine the design and the concept of operations of the former LAPCAT-II MR2.4 vehicle, and to reach the ambitious goal of TRL=6 by 2035 for the concept, considering that the crucial technologies of STRATOFLY MR3 vehicle may represent a step forward to reach the goal of future reusable space transportation systems, drastically reducing transfer time (i.e. antipodal flights in less than two to four hours), emissions and noise, and guaranteeing the required safety levels. STRATOFLY MR3 vehicle presents a highly integrated structure which is characterized by a complex waverider configuration with dorsal mounted propulsive subsystem. Aerodynamic forces and propulsive thrust are strictly interdependent and need to be calculated with complete simulations that consider both external and internal flow path and in addition the detailed combustion process and the pollutants emission.

In this framework an aeropropulsive characterization of the MR3 hypersonic cruiser configuration was conducted in order to mainly compute and verify the amount of thrust required at cruise conditions (Mach=8). In order to do this both engineering tools (SPREAD) and detailed CFD computations have been conducted and several configurations of the combustion chamber have been analyzed. In particular, the aim of the present activity has been the aerodynamic characterization of the isolator part of STRATOFLY combustion chamber for what concerns its effect on the combustion process and, in particular, the possible back interaction with the air flow capturing operated by means of the intake part and, in general, to verify the correct capturing of air flow. This has been characterized by simulating a configuration that considers the following parts: INTAKE, ISOLATOR, COMBUSTOR, STRUTS and, if the case, a part of the nozzle. Another aim was to obtain a characterization of pollutants emission.

**Keywords:** Hypersonic vehicle, Aero-thermodynamic Characterization; Hypersonic civil transport, Hydrogen Combustion, Scramjet Propulsion, Stratofly

## 1. Introduction

The H2020 STRATOFLY Project is a highly-multidisciplinary project co-funded by the European Commission that combines technological and operative issues for hypersonic civil aircrafts and aims to study the feasibility of high-speed passenger stratospheric flight. The main objectives were to refine the design and the concept of operations of the former LAPCAT-II MR2.4 vehicle, and to reach the ambitious goal of TRL=6 by 2035 for the concept, considering that the crucial technologies of STRATOFLY MR3 vehicle (Figure 1) may represent a step forward to reach the goal of future reusable space transportation systems. Technological, environmental, operational and economic factors, that allow the global sustainability of new air space's exploitation, are considered, drastically reducing transfer time (i.e. antipodal flights in less than two to four hours), emissions and noise, and guaranteeing the required safety levels. In addition to the wide range of flight conditions to be considered, STRATOFLY MR3 presents a highly integrated structure which is characterized by a complex waverider configuration with dorsal mounted propulsive subsystem. Aerodynamic forces and propulsive thrust are strictly interdependent and need to be calculated with complete simulations that consider both external and internal flow path and in addition the detailed combustion process and the pollutants emission.



Figure 1 – The STRATOFLY MR3 hypersonic cruiser.

In the framework of the H2020 STRATOFLY project, an aero-propulsive characterization of the MR3 hypersonic cruiser configuration was conducted in order to mainly compute and verify the amount of thrust required at cruise conditions (Mach=8). In order to do this both engineering tools (SPREAD) and detailed CFD computations have been conducted and several configurations of the combustion chamber have been analyzed. In particular, the aim of the present activity has been the aerodynamic characterization of the isolator part of STRATOFLY combustion chamber for what concerns its effect on the combustion process and, in particular, the possible back interaction with the air flow capturing operated by means of the intake part and, in general, to verify the correct capturing of air flow. This has been characterized by simulating a configuration that considers the following parts: INTAKE, ISOLATOR, COMBUSTOR, STRUTS and, if the case a part of the nozzle. Another aim was to obtain a characterization of pollutants emission.

## 2. CFD Simulations of Intake-Combustor-Struts Configuration

### 2.1 Test Matrix

The basic CFD test matrix (see Table 1) is composed of three groups of numerical simulations.

Table 1: Basic CFD Test Matrix

configuration		MACH					
		3	4	5	6	7	8
baseline	non reacting	VKI	CIRA	VKI	CIRA	VKI	CIRA
optimized	non reacting		CIRA				CIRA
optimized	reacting		CIRA				CIRA

The baseline-non-reacting group of simulations is mainly aimed at verifying the correct working of the system composed of intake and the combustor chamber with the presence of struts in terms of a good air flow capturing without choking of the entire process. This activity has also given input to the 1D reacting tools that have to provide the DMR engine thrust for the Aero Propulsive Database development and the combustion products for the environmental impact calculations.

The optimized-non-reacting group of simulations is aimed at verifying the correct working of the internal flow with a configuration where the struts are allocated at the end of the combustor, and always to give input for the 1D calculations of reacting flow similarly to the first group of simulations (Figure 2).

The final optimized-reacting group are the reacting flow simulations of the previous group. The aim is to obtain three-dimensional full reacting simulations in order to mainly verify the emission index of NO (EINO) and to compare it with the results obtained for the baseline-reacting combustor configuration obtained during LAPCAT-II project.

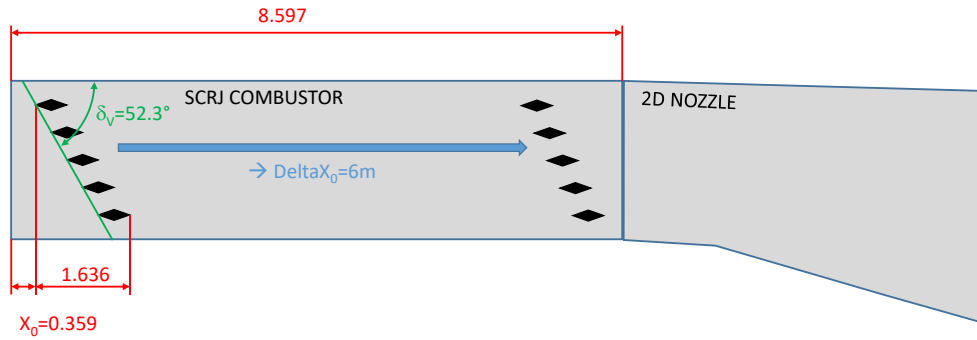


Figure 2 – Struts Location along the Combustor Chamber.

## 2.2 Baseline Non-Reacting Configuration

The baseline configuration (see Figure 3) is composed of:

- Intake
- Combustor channel
- Struts (23 and more than 1200 holes in full configuration for the Hydrogen  $H_2$  injection)
- Part of the external fuselage (up to the end of combustor)

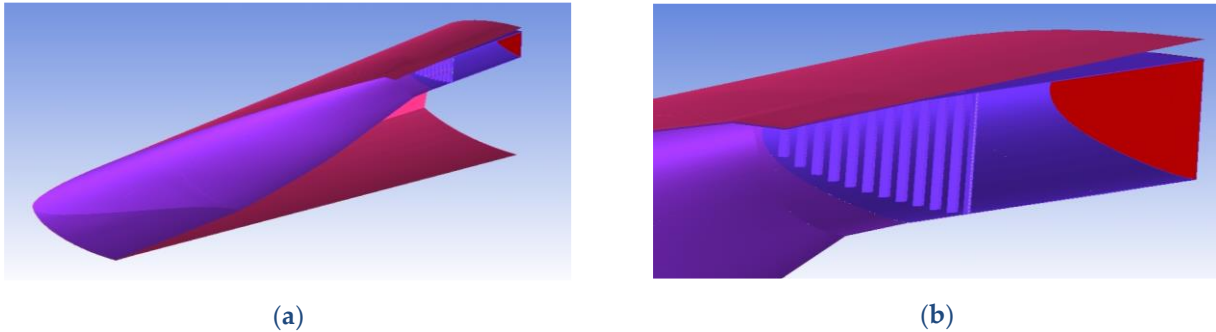


Figure 3 – Baseline configuration.

Being the geometry very complex for the presence of a very high number of  $H_2$  injection holes, an unstructured approach has been selected for the grid generation. So, the commercial ANSYS tools have been used for this analysis: ICEMCFD-TETRA for grid generation and FLUENT for fluid flow calculations.

After some initial trials to obtain a not so huge numerical grid (i.e., to reduce convergence time) for the whole geometry, it was decided to proceed with a hybrid approach. The geometry has been divided into two parts:

- External: Fuselage + Intake up the combustor inlet
- Internal: Combustor + Struts

Then, the two grids have been generated separately and joint together with non-conformal interface directly inside the FLUENT CFD code.

Main characteristics of the grid for boundary layer are:

- $\Delta y_{wall} = 0.15 \text{ mm} = 1.5 \cdot 10^{-4} \text{ m}$
- 10 Layers
- Total height = 10.472 mm

The obtained total number of cells is about 30 million, see Figure 4.

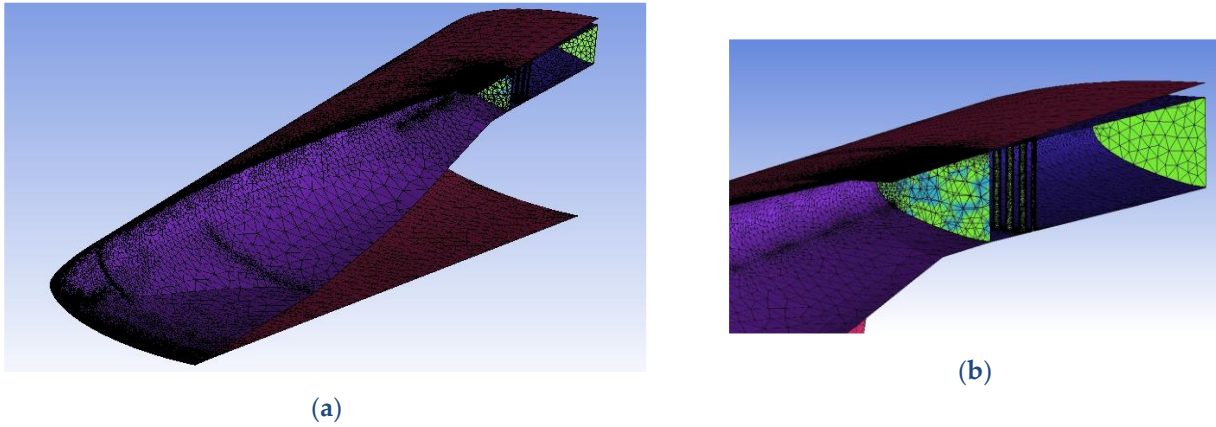


Figure 4 – Grid for baseline configuration.

Table 2: Far Field Conditions

ALTITUDE [km]	MACH [ ]	P_ATM [Pa]	P_TOT [Pa]	RHO_ATM [kg/m3]	TEMP_ATM [K]	TEMP_RIST [K]	OUND_SPEE [m/s]	VELOCITY [m/s]	S_inflow [m2]	S_outflow [m2]	MFR inflow [kg/s]
32.30	8.000	845.10	8250588.06	0.01322	222.70	3073.26	299.13	2393.07	37.573	4.970	1188.89
29.94	7.000	1187.00	4913985.42	0.01792	230.80	2492.64	304.52	2131.67	37.573	4.970	1435.28
26.00	6.000	2152.68	3398821.55	0.03369	222.65	1825.73	299.10	1794.60	37.573	4.970	2271.56
24.44	5.000	2794.80	1478700.13	0.04426	220.00	1320.00	297.31	1486.57	37.573	4.970	2472.37
21.00	4.000	4668.99	708916.66	0.07509	216.65	909.93	295.04	1180.17	37.573	4.970	3329.72

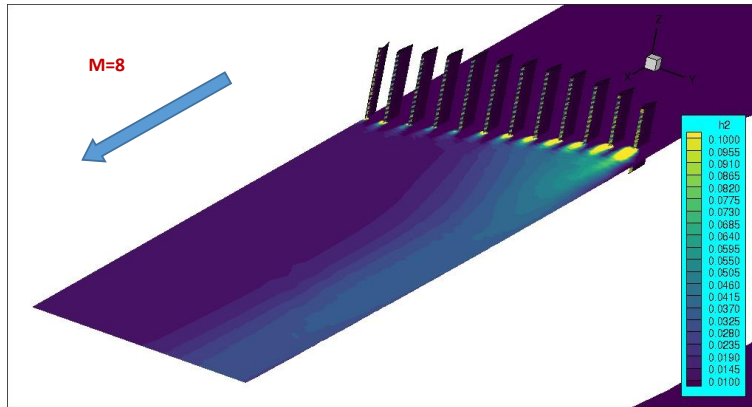
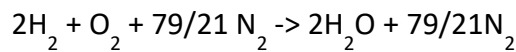


Figure 5 – Iso-contour of H2 for the non-reacting Mach=8 case.

From Figure 4 is possible to see the non-conformal interface just before the struts. A simple chemical scheme (CHEMKIN format) has been used for the non-reacting cases where Oxygen, Nitrogen and Hydrogen are imported into FLUENT.

In order to set the correct boundary conditions at injection holes, it is the case to recall some definitions of chemical and aerothermodynamic quantities.

From the chemical reaction between air and hydrogen (with a neutral nitrogen) it yields:



So, the stoichiometric ratio between air and hydrogen can be easily derived:

$$\frac{\dot{m}_{air}}{\dot{m}_{fuel}} = \frac{\frac{79}{21} * 28 + 1 * 32}{2 * 2} = \frac{2884}{84} = 34.2$$

And the inverse one, too:

$$\frac{\dot{m}_{fuel}}{\dot{m}_{air}} = 0.02924$$

The Equivalence Ratio (ER) is defined as the ratio of the actual fuel-air ratio to the stoichiometric one:

$$\varphi = ER = \frac{\left(\frac{\dot{m}_{fuel}}{\dot{m}_{air}}\right)_{actual}}{\left(\frac{\dot{m}_{fuel}}{\dot{m}_{air}}\right)_{stoich}}$$

The relation between the Mass Flow Rate (MFR) at the end of the nozzle and the stagnation quantities is:

$$MFR = \frac{P_0 * A^*}{\sqrt{T_0}} * \sqrt{\frac{\gamma}{R} * \left(\frac{2}{\gamma + 1}\right)^{(\gamma+1)/(\gamma-1)}}$$

where:

$$P_0 = P * \left(1 + \frac{\gamma - 1}{\gamma} * M^2\right)^{\gamma/(\gamma-1)}$$

Full boundary condition (BC) Settings Procedure:

- Run w/o injection (or with a trial injection). (Conditions of Table 2).
  - Extract air flow rate, P, T from entrance of combustor. (4<sup>th</sup> column of Table 3 for MFR and values of Table 5).
  - Estimate of thrust with simplified methods, and so ER. (7<sup>th</sup> column of Table 3)
  - Calculate fuel mass flow rate ER formula. (Last column of Table 3)
  - Calculate fuel pressure at injection nozzle (Mach=3) from isentropic formulae. (Last column of Table 4).
  - Split of H<sub>2</sub> MFR between holes up and down (1<sup>st</sup> and 2<sup>nd</sup> columns of Table 3)
- Holes-up and holes-down are two different groups of holes located on the two sides of struts (y-positive-wise, y-negative-wise).

Table 3: Quantities extracted from non-reacting simulations

holes down	holes up	Mach	MFR air inpit	MFR air id.	Eff capt.	ER	mfr ratio st	mfr H2
5.57849	5.19443	8.00	567.6946	594.45	0.95	0.649000	0.02924	10.77292
5.88318	5.47814	7.00	665.3373	717.64	0.93	0.584000	0.02924	11.36132
6.54383	6.09331	6.00	982.2501	1135.78	0.86	0.440000	0.02924	12.63714
3.06794	2.85672	5.00	993.2526	1236.19	0.80	0.204000	0.02924	5.92466
3.79580	3.53447	4.00	1179.0595	1664.86	0.71	0.212623	0.02924	7.33027

Table 4: Settings at injection holes.

Mach	ER	MFR	Mex nozz	P0	T0	Pex
8.00	0.6490	10.77964	3	7499998.98	800	204177.6
7.00	0.5840	11.36132	3	7904703.52	800	215195.1
6.00	0.4400	12.63714	3	8792362.51	800	239360.5
5.00	0.2040	5.92466	3	4122120.84	800	112219.3
4.00	0.2126	7.33027	3	5100077.84	800	138842.9

Table 5: Input for 1D calculations

MACH FF	MACH	P	TEMP	rho	Vel
[ ]	[ ]	[Pa]	[K]	[Kg/m3]	[m/sec]
8	3.604	29719.972	877.190	0.113513	2076.365
7	3.235	36720.393	813.890	0.151298	1829.257
6	2.789	57472.389	722.846	0.274397	1477.354
5	2.280	65602.560	647.898	0.353245	1158.244
4	1.610	106825.680	598.583	0.620542	781.848

In general, since the flight trajectory can change, the above CFD extracted value have to be adapted to the actual trajectory (Figure 6). In the pictures below, it is presented an example of adaptation from the CFD to the actual and reference trajectory when these calculations have been done.

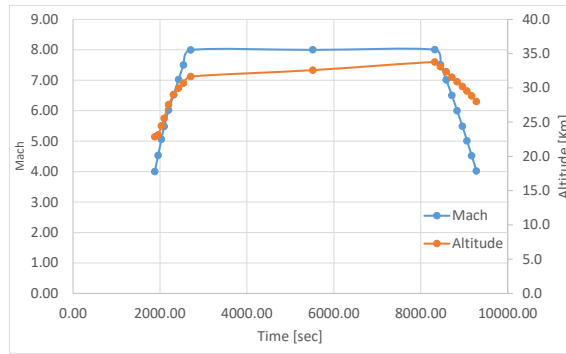


Figure 6: Nominal trajectory in the range Mach=4-8.

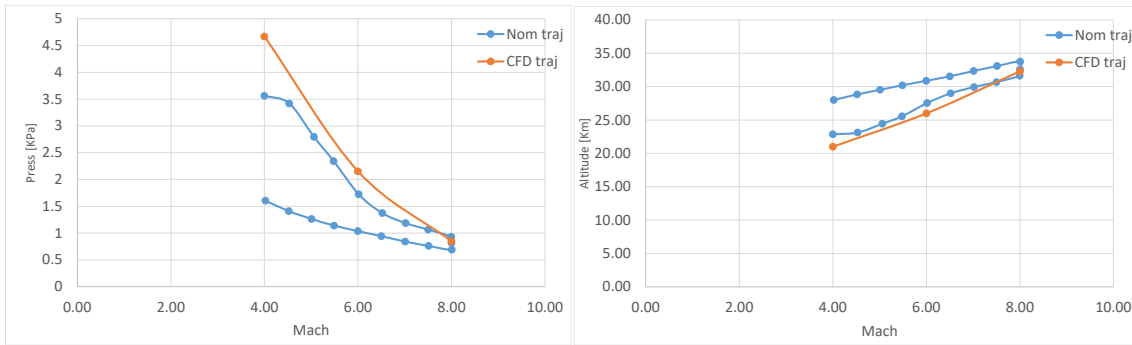


Figure 7: Pressure and Altitude. CFD vs. Nominal trajectory.

Once we have the CFD results, combustor conditions (both air and H<sub>2</sub>) can be scaled with flight ones (Table 6), and results are shown in Figure 8 and Figure 9. It must be remarked that the Mach number at the combustor's entrance is kept unchanged since it only depends on the geometry of air intake (in this case, neglecting Reynolds number effect).

Table 6: Values at the entrance of combustor adapted/scaled to the nominal trajectory

MACH FF	MACH	P	TEMP	rho	Vel	MFR half
[ ]	[ ]	[Pa]	[K]	[Kg/m3]	[m/sec]	[Kg/sec]
4.00	1.610	81534.552	604.582	0.469899	793.560	906.7170
5.00	2.280	65603.036	649.009	0.352202	1164.359	997.1627
6.00	2.789	46024.102	733.832	0.218528	1514.673	804.8461
7.00	3.235	36720.393	813.890	0.157203	1849.933	707.1365
8.00	3.604	32690.665	929.156	0.122590	2202.340	656.4856
8.00	3.604	28683.791	942.653	0.106024	2218.279	571.8817
8.00	3.604	24264.770	958.107	0.088243	2236.388	479.8604
7.00	3.235	26071.100	840.177	0.108120	1879.571	494.1430
6.00	2.789	27697.854	758.321	0.127266	1539.738	476.4809
5.00	2.280	29673.627	677.278	0.152659	1189.448	441.5240
4.00	1.610	36727.413	627.046	0.204084	808.168	401.0500

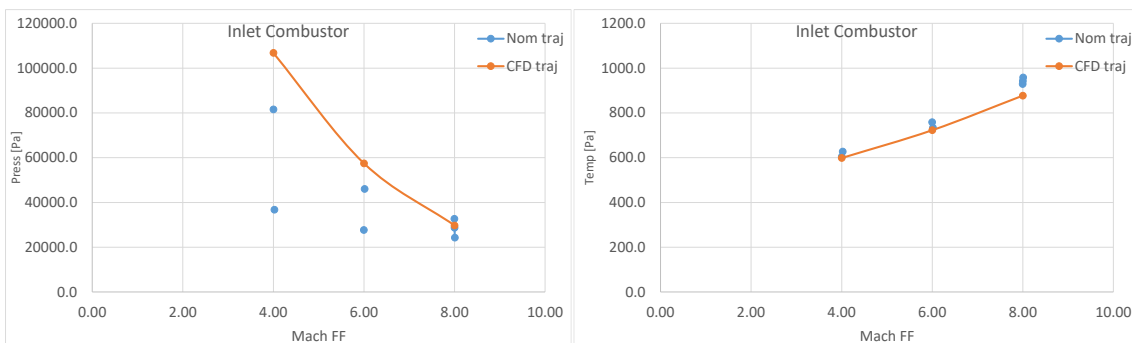


Figure 8: Pressure and Temperature at entrance of Combustor.

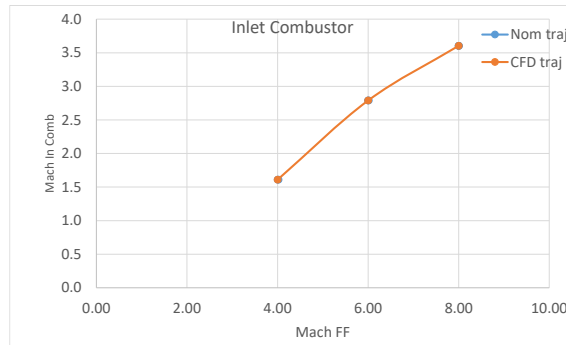


Figure 9: Mach number at entrance of Combustor.

### 2.3 Optimized Non-Reacting Configuration

For the optimized combustor's configuration, an analogous procedure was pursued for the grid generation, operating for the external and internal parts separately. In this case since the struts are located at the end of combustor, a part of the nozzle (2D nozzle) has been added (see Figure 10 and Figure 11). The total number of cells still remains of about 30 million. The exploitation of these CFD simulations, for what concerns the 1D activities, occurs in the same way as described in the previous sub-section.

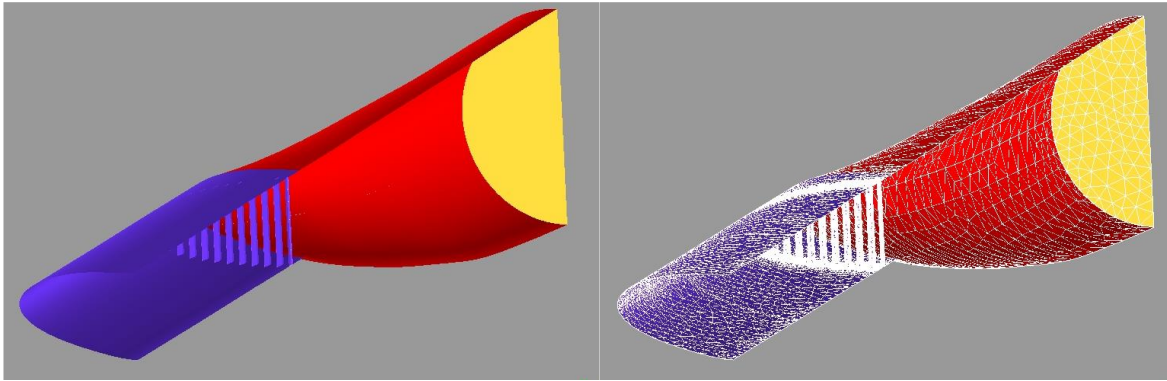


Figure 10: Geometry and grid for the internal part.

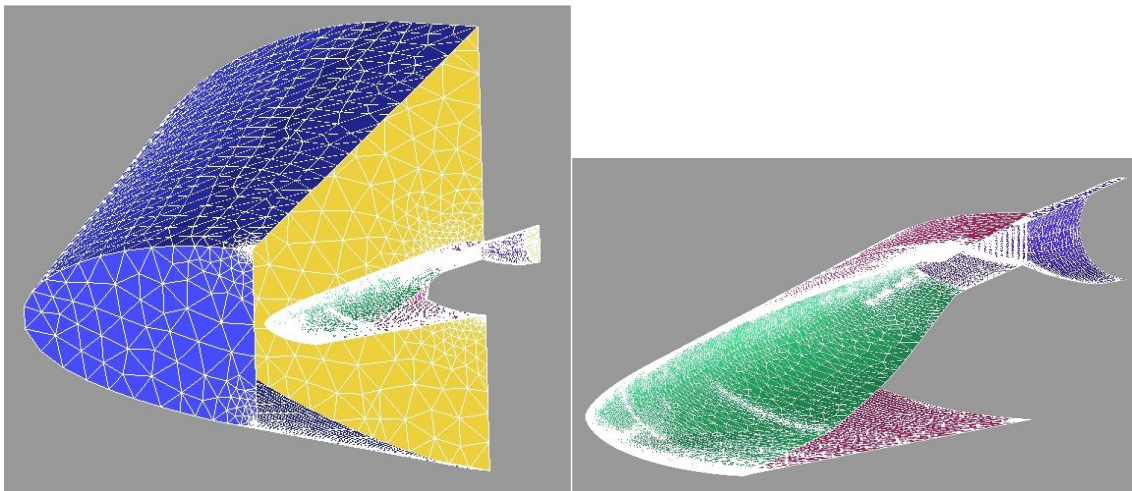


Figure 11: Grid for external part. The left picture shows also the far field boundaries.

### 2.4 Optimized Reacting Configuration

For the reacting cases of Table 1, the Mach 8 and Mach 5 (instead of Mach 4, as stated at the beginning) far field conditions have been considered.

For the chemical kinetics of air-hydrogen combustion, the Jachimowski reduced scheme of Table 7, verified and validated in LAPCAT-II project for scramjet engine conditions, has been used in conjunction with the EDC (Eddy Dissipation Concept) model of FLUENT code.

Table 7: Reduced Jachimowski chemical scheme. 9 species and 12 reactions

ELEMENTS	H	O	N	END										
SPECIES	H2	O2	H2O	N2	H	O	OH	N	NO	END				
REACTIONS														
H+OH+M=H2O+M										0.221E+23	-2.00	0.0	!1	!processo di combustione
H2O/16.0/ H2/2.5/														
H+H+M=H2+M										0.730E+18	-1.0	0.0	!2	!processo di combustione
H2O/16.0/ H2/2.5/														
H2+O2=OH+OH										0.170E+14	0.0	48000	!3	!processo di combustione
H+O2=OH+O										0.120E18	-0.91	16512	!4	!processo di combustione
OH+H2=H2O+H										0.220E+14	0.0	5150	!5	!processo di combustione
O+H2=OH+H										0.506E+5	2.67	6290	!6	!processo di combustione
OH+OH=H2O+O										0.630E+13	0.0	1090	!7	!processo di combustione
N+N+M=N2+M										2.80E+17	-0.8	0.0	!8	!dissociazione dell'N2
H2/2.5/ H2O/16.0/														
O+O+M=O2+M										1.10E+17	-1.0	0.0	!9	!dissociazione dell'O2
H2/2.5/ H2O/16.0/														
N+O2=NO+O										6.40E+9	1.0	6300	!10	!seconda di Zel'dovich
N+NO=N2+O										1.60E+13	0.0	0.0	!11	!prima di Zel'dovich
N+OH=NO+H										6.30E+11	0.5	0.0	!12	!terza di Zel'dovich
END														

Contours of nitrogen oxide and water vapor are reported in Figure 12 on symmetry plane. A stratification can be noted for the NO distribution mainly located in the lower part of the nozzle while the H<sub>2</sub>O seems to be more widespread. Figure 13 shows the contour of temperature at several transversal sections all along the combustor chamber and nozzle.

Figure 14 and Figure 15 show average values along the combustor chamber and 2D nozzle are reported. It must be noted the strong increase of temperature and pressure and the strong decrease of Mach number in the struts zone where a sudden combustion of H<sub>2</sub> happens.

The distribution of EINO (reported in Figure 16) shows a strong increase in the struts/combustion zone while remains nearly constant in the nozzle where the temperature starts decreasing.

In Figure 16 it is possible to see a comparison of EINO distribution for STRATOFLY MR3 and LAPCAT-II MR2.4 vehicles. The beneficial effect of shifting backward the strut array can be clearly appreciated, with an overall EINO value reduction of roughly 50% at nozzle exhaust.

Nevertheless, the combustion efficiency remains very high for the optimized configuration as it can be seen from Figure 17 where a comparison with LAPCAT-II MR2.4 case is also reported.

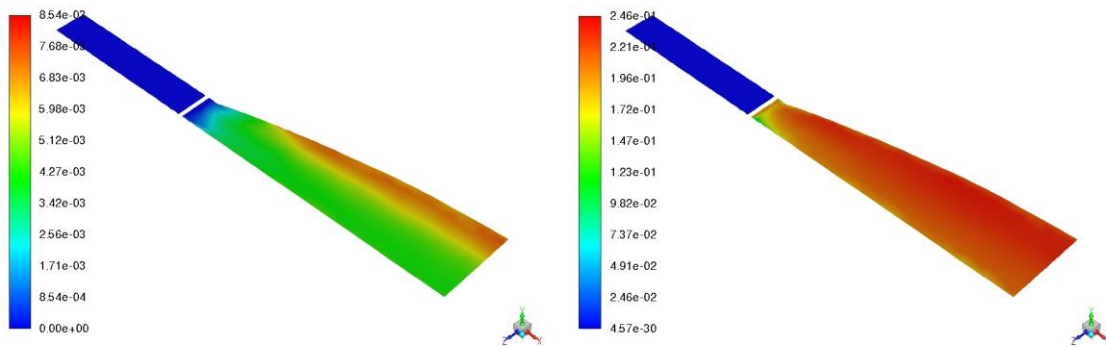


Figure 12: Mass fraction of NO and H<sub>2</sub>O on the symmetry plane (internal part). Mach=8.

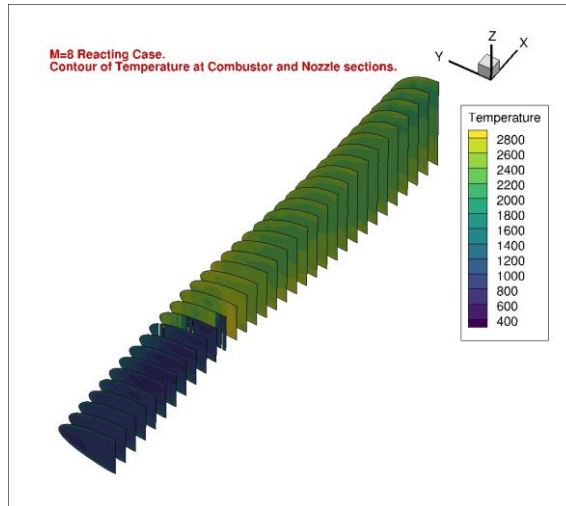


Figure 13: Contour of Temperature at Combustor and Nozzle sections. Mach=8 reacting case.

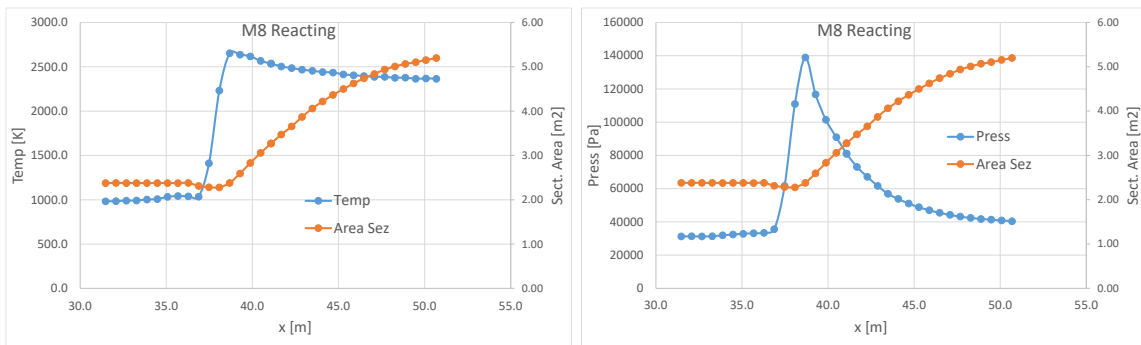


Figure 14: Average Temperature and Pressure along combustor and nozzle. Mach=8 reacting.

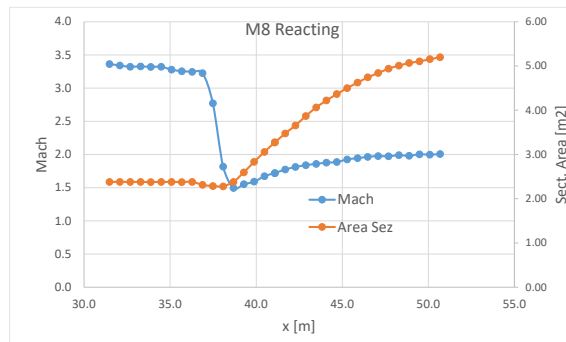


Figure 15: Average Mach number along combustor and nozzle. Mach=8 reacting.

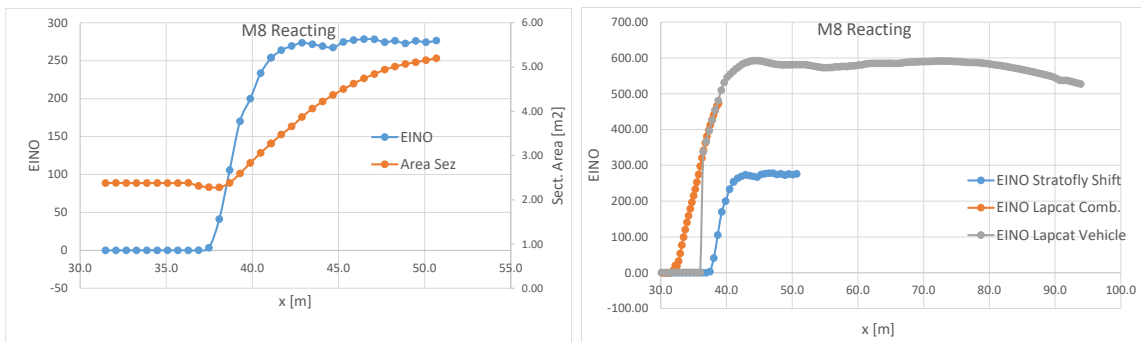


Figure 16: EINO along combustor and nozzle. Mach=8 reacting on the left. Comparison with LAPCAT-II MR2.4 case, combustor stand alone and full vehicle (3D/3D coupling) on the right.

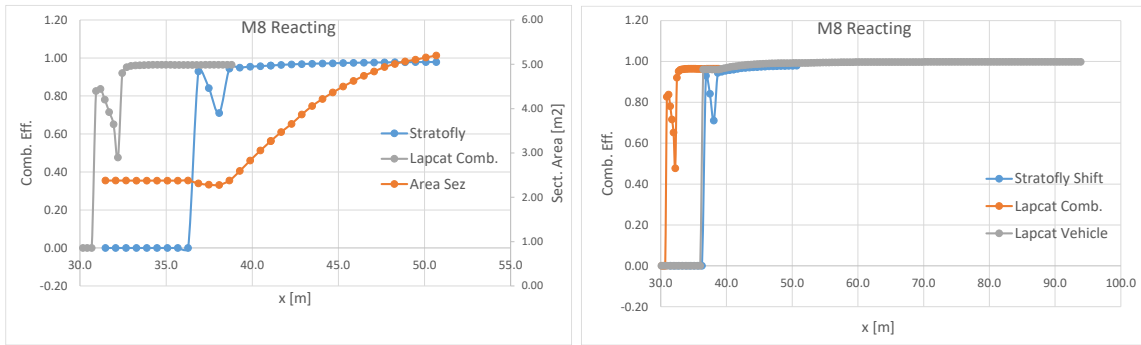


Figure 17: Combustion Efficiency along combustor and nozzle. Mach=8 reacting. Comparison with LAPCAT-II MR2.4 combustor on the left. Comparison with LAPCAT-II MR2.4 case, combustor stand alone and full vehicle (3D/3D coupling) on the right.

### 3. SPREAD Validation through comparison with CFD

The main objective of the CFD simulations just shown has been to characterize the isolator at a better level of accuracy than what was done during the LAPCAT-II project (in which the isolator was not really modeled at all). At the beginning of the STRATOFLY project, the SPREAD engineering tool was equipped with a simplified module for the evaluation of the pressure and temperature jumps through the struts array with the simultaneous injection of hydrogen: this module, however, needs, as input, the values of Mach pressure and temperature immediately upstream of the array, which derive from the air intake but which are strongly influenced by the presence of the struts array itself and the consequent shock wave trains that are generated in the isolator when this component is long enough: the conditions so determined were not available at the end of the LAPCAT-II project and not even at the beginning of the STRATOFLY project; for this reason, instead of using the conditions immediately upstream of the array, the conditions at the end of the air intake were used, i.e. considering null any variations in the isolator.

But now, given the non-reactive CFD simulations here presented, the input values of pressure, temperature and Mach number in the immediately upstream section of the struts array are available, thus they can be used by SPREAD for more accurate evaluations. In particular, the optimized configuration of Dual-Mode Ramjet (DMR) engine was analyzed, i.e. the one in which the struts array is moved 6 meters downstream, and then compared with the CFD area-averaged results.

Figures 18 and Figure 19 report the comparison between the CFD area-averaged and SPREAD results, for temperature, pressure, Mach number and EINO index: the very good agreement for all the quantities confirms the reliability of the SPREAD code, as long as it is fed with the correct input data. As a further confirmation, Figure 20 also shows the comparison, in terms of the EINO index, between the CFD results of LAPCAT-II MR2.4 vehicle (red and orange curves) and the preliminary analyzes conducted at the beginning of the STRATOFLY project on the LAPCAT-II vehicle (brown curve, identified with the SPREAD LAPCAT-II label): as explained above, the comparison between CFD and SPREAD is here worse because any effects of the isolator on the determination of the input data are missing.

Finally, again in Figure 20, the EINO profile is shown, in green, for the STRATOFLY MR3 nominal configuration (for which a complete reacting simulation is currently lacking); a reduction of about 65% of the EINO index is expected when the optimized configuration is adopted for MR3 vehicle (in blue and light blue).

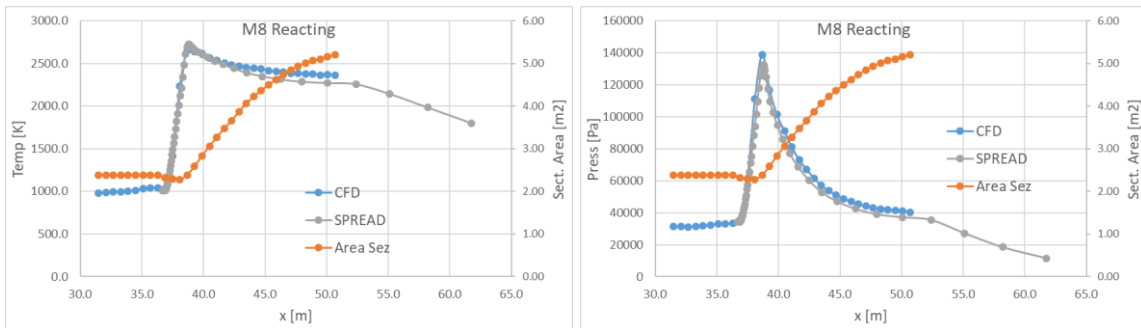


Figure 18: CFD vs. SPREAD Average Temperature and Pressure along combustor and nozzle. Mach=8 reacting.

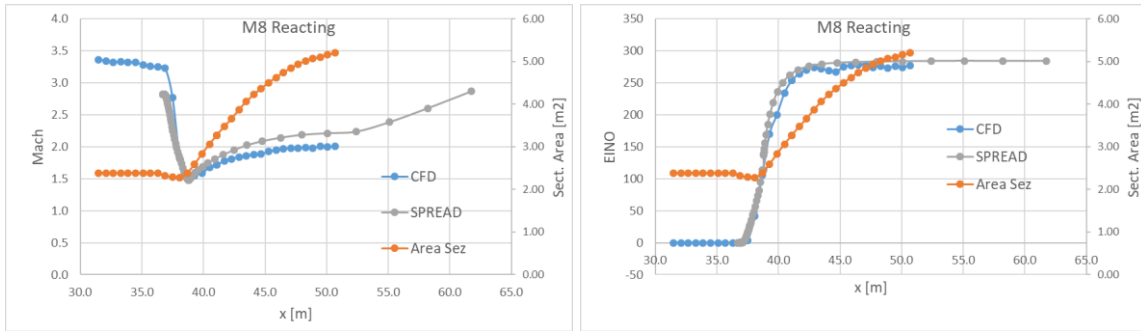


Figure 19: CFD vs. SPREAD Average Mach and EINO Index number along combustor and nozzle. Mach=8 reacting.

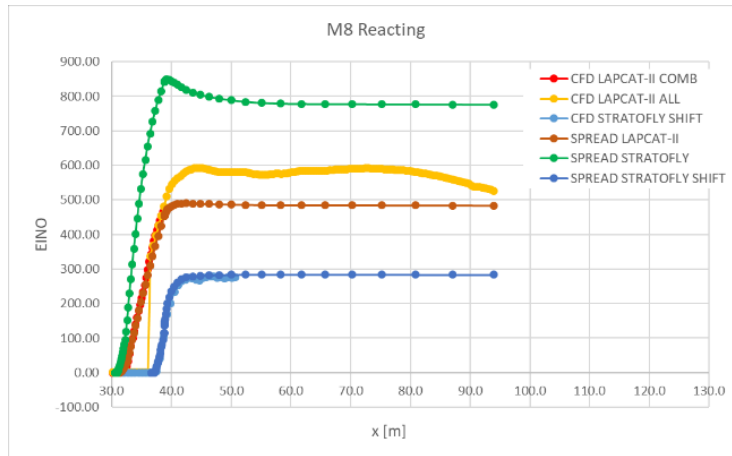


Figure 20: CFD vs. SPREAD: comparison between LAPCAT-II MR2.4 and STRATOFLY MR3.

#### 4. Conclusions

In this paper an analysis of the propulsive balance of the STRATOFLY MR3 vehicle has been reported. By using the engineering code SPREAD with improved modelling capabilities and a large number of high-fidelity CFD simulations, an optimized DMR combustor for the MR3 vehicle has been defined, shifting the baseline strut array of about 6m towards the end of combustor, and keeping unchanged the angle of the V-shape structure of the struts array.

The CFD simulations of the complete propulsive flowpath performed, both for the baseline DMR combustor and for the optimized DMR combustor, allowed delivering more reliable inputs (especially for the “isolator” region) to the 1D reacting tool (SPREAD) that has to provide the DMR engine thrust for the Aero Propulsive Database development and the combustion products (NO, H<sub>2</sub>O) for the environmental impact calculations. So, SPREAD engineering tool has been validated through comparison with these new CFD results, and immediately used also to assess the beneficial effect on EINO of flying at higher cruise altitude (36km instead of 32km). Present results of STRATOFLY MR3 vehicle have been always compared to the results obtained during LAPCAT-II project for the older MR2.4 vehicle, and the obtained EINO reduction with keeping propulsive performance has been highlighted.

#### 5. Copyright Statement

The authors confirm that they, and/or their company or organization, hold copyright on all of the original material included in this paper. The authors also confirm that they have obtained permission, from the copyright holder of any third party material included in this paper, to publish it as part of their paper. The authors confirm that they give permission, or have obtained permission from the copyright holder of this paper, for the publication and distribution of this paper as part of the ICAS proceedings or as individual off-prints from the proceedings.

#### Acknowledgment

This work has been carried out within the frame of “MDO and REgulations for Low boom and Environmentally Sustainable Supersonic aviation” (MORE&LESS) project. This project has received funding from the European Union’s Horizon 2020 research and innovation program under grant agreement No 101006856.

#### References

- [1] Raymer, D. P., “Aircraft design: a conceptual approach”, edited by J. A. Schetz, 6<sup>th</sup> Edition, AIAA Education Series, AIAA, Reston (VA), 2018. <https://doi.org/10.2514/4.104909>

- [2] Viola, N., Fusaro, R., Gori, O., Marini, M., Roncioni, P., Saccone, G., ... & Bodmer, D. (2021). STRATOFLY MR3– how to reduce the environmental impact of high-speed transportation. In AIAA Scitech 2021 Forum (p. 1877).
- [3] Ferretto, D., Fusaro, R., & Viola, N. (2020). A conceptual design tool to support high-speed vehicle design. In AIAA AVIATION 2020 FORUM (p. 2647).
- [4] Schlichting, H., *Boundary Layer Theory*, McGRAW-HILL, 1979.
- [5] Deng, A., *Aerodynamic Performance Prediction of SpaceShipTwo*, December 2012, DOI: 10.13140/RG.2.1.3540.4885
- [6] Steelant, J., Varvill, R., Defoort, S., Hannemann, K., Marini, M., “Achievements Obtained for Sustained Hypersonic Flight within the LAPCAT-II Project”, 20th AIAA International Space Planes and Hypersonic Systems and Technologies Conference, Glasgow, Scotland, AIAA-2015-3677, 2015.
- [7] Martinez Schramm J., Hannemann K., Laurence S., Karl S., “Ground based testing of complete M8 flight experiment configuration in HEG”, deliverable D5.2.5, LAPCAT-II Project, ACP7-GA-2008-211485, 2014.
- [8] Langener T., Karl S., Dupont B., Roncioni P., Ferrier M., “Nose-to-tail CFD analysis of the subscale M8 flight configuration”, deliverable D3.4.4, LAPCAT-II Project, ACP7-GA-2008-211485, 2014.
- [9] Piscitelli, F., Cutrone, L., Pezzella, G., Roncioni, P., Marini, M., “Nose-to-tail analysis of an airbreathing hypersonic vehicle using an in-house simplified tool”, *Acta Astronautica*, Vol. 136, pp. 148-158, 2017.